Supporting Information

Fabrication of light-responsive polymer nanocomposite containing spiropyran as sensor for reversible recognition of metal ions

Fakhri Arjmand, Zahra Mohamadnia*

Polymer Research Laboratory, Department of Chemistry, Institute for Advanced Studies in Basic Science (IASBS), Gava Zang, Zanjan, 45137-66731, Iran

Email address: z.mohamadnia@iasbs.ac.ir

1. Characterization

An Agilent 1100 series instrument was used to perform gel permeation chromatography (GPC) analysis in THF solvent to determine the molecular weight of the surface-grafted polymer and free polymer. FT-IR Bruker Vector 22 spectrophotometer (Germany) at room temperature was employed for identification of the functional groups of all synthesized compounds in the range of 450-4000 cm^{-1}, using KBr pellets. The structure of all synthesized organic compounds and polymer was further confirmed by nuclear magnetic resonance (NMR) BRUKER 400MHz instrument (Germany) in $CDCl_3$ and d_6-DMSO solvents. Melting points were measured by the Thermo scientific 9200 (England). Thermogravimetric analysis (TGA) was carried out in an N_2 atmosphere with a heating rate of 10 °C/min (from RT to 600 °C) by NETZSCH STA 409 PC/PG (Germany) to evaluate the thermal stability of the synthesized compounds. The content of amine, bromine, and the grafted polymer on the surface of TiO_2 was also measured through TGA. The surface area of the nanoparticles was estimated at 77 K using a Belsorp-max, BEL, Inc instrument, according to the Brunauer–Emmett–Teller theory (BET) (Japan). The morphology and size of the pure and surface-modified TiO_2 were determined using atomic force microscopy (AFM, Ara-Research CO). UV-Vis analysis using the Pharmacia Ultrospec Biotech 4000 under license Biochrom Ltd. Cambridge (England) was used to study the photochromic characteristics of the produced substances. The copolymers in solid-state were mixed with barium sulfate (1:25) and their photochromic properties were identified by UV-Vis-NIR spectrophotometer (CARY 5E, Varian America). The percentage of elements in the combination of pure TiO_2 nanoparticles and TiO_2-*g*-P(SPEA-*co*-GMA) was determined by Energy dispersive X-ray (EDS) mapping analysis (MIRA II, SAMX detector, Czechia). It should be noted that the samples were exposed to ultraviolet and visible light at each step.

2. Purification

2.1. Toluene [1]

First, toluene was slowly distilled at 110° C. Then, the sodium wire was put to the distilled solvent for complete drying, carefully. To validate the drying of toluene, a benzophenone detector was added to the solvent, and the solution was distilled under argon atmosphere for several days (typically 3 days), and the process was repeated until the solution turned blue. This discoloration indicated that the toluene had dried completely.

2.2. Ethanol [1]

Powdered and dry magnesium (5 g) with iodine (0.5 g) entered into a 2L flask and absolute ethanol (about 50-75 mL) was slowly added to the flask and with increasing temperature, all the magnesium converted to magnesium ethoxide. More than 1 L of the absolute ethanol was added to the flask and refluxed overnight under argon atmosphere. When magnesium hydroxide precipitates, the ethanol is completely dry.

2.3. Dichloromethane [1]

$CaCl_2$ was added to dichloromethane and distilled under argon atmosphere. The distilled dichloromethane was then added to a container containing CaH_2 and returned under distillation under argon atmosphere.

2.4. Copper bromide [2, 3]

Copper bromide (CuBr) was purified by rinsed frequently with acetic acid until the color of the supernatant solution was very light, then allowed to stir for overnight in a closed container at room temperature. Followed by removing the acetic acid, absolute ethanol was added to it and rinsed. After separation, CuBr drying in a vacuum at 60 ° C overnight.

3. Synthesis of monomer [4]

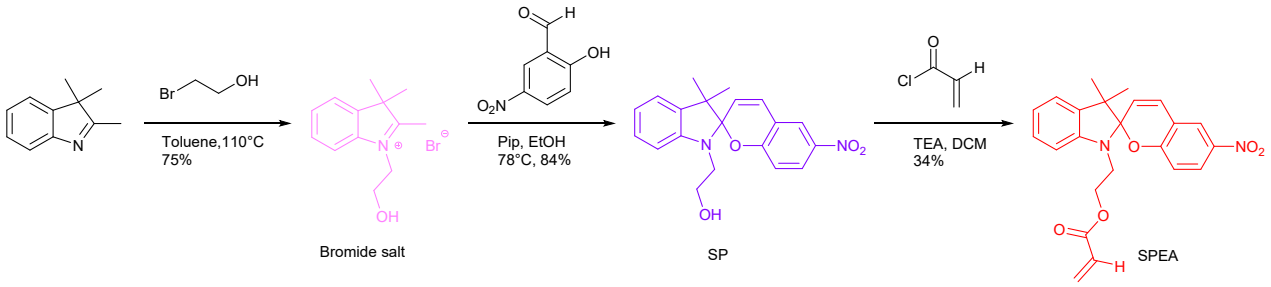

Scheme S1. Synthesis method for preparation of SPEA

3.1. Synthesis of 1-(2-hydroxyethyl)-2,3,3-trimethyl-3H-indol-1-ium bromide (Bromide salt).

2,3,3-Trimethyl indoline (3 mL, 18.69 mmol) and dry toluene (30 mL) were mixed in round-bottom flask (Scheme S1). 2-Bromoethanol (1.61 mL, 22.80 mmol) was added to the reaction mixture and refluxed for 24 h. After the reaction was completed, the mixture was placed at room temperature and precipitate was washed with cold toluene to obtain bromide salt as light pink solid salt (3.9 g, 75%).

Bromide salt: (284.192 $g.mol^{-1}$, melting point: 197 °C)

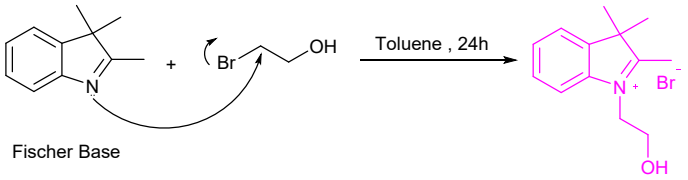

Scheme S2. Synthesis mechanism of 1- (2-hydroxyethyl) -2,3,3-trimethyl-3H-indol-1-ium bromide (Bromide salt)

3.1.1. ^{1}H NMR and ^{13}C NMR of Bromide salt

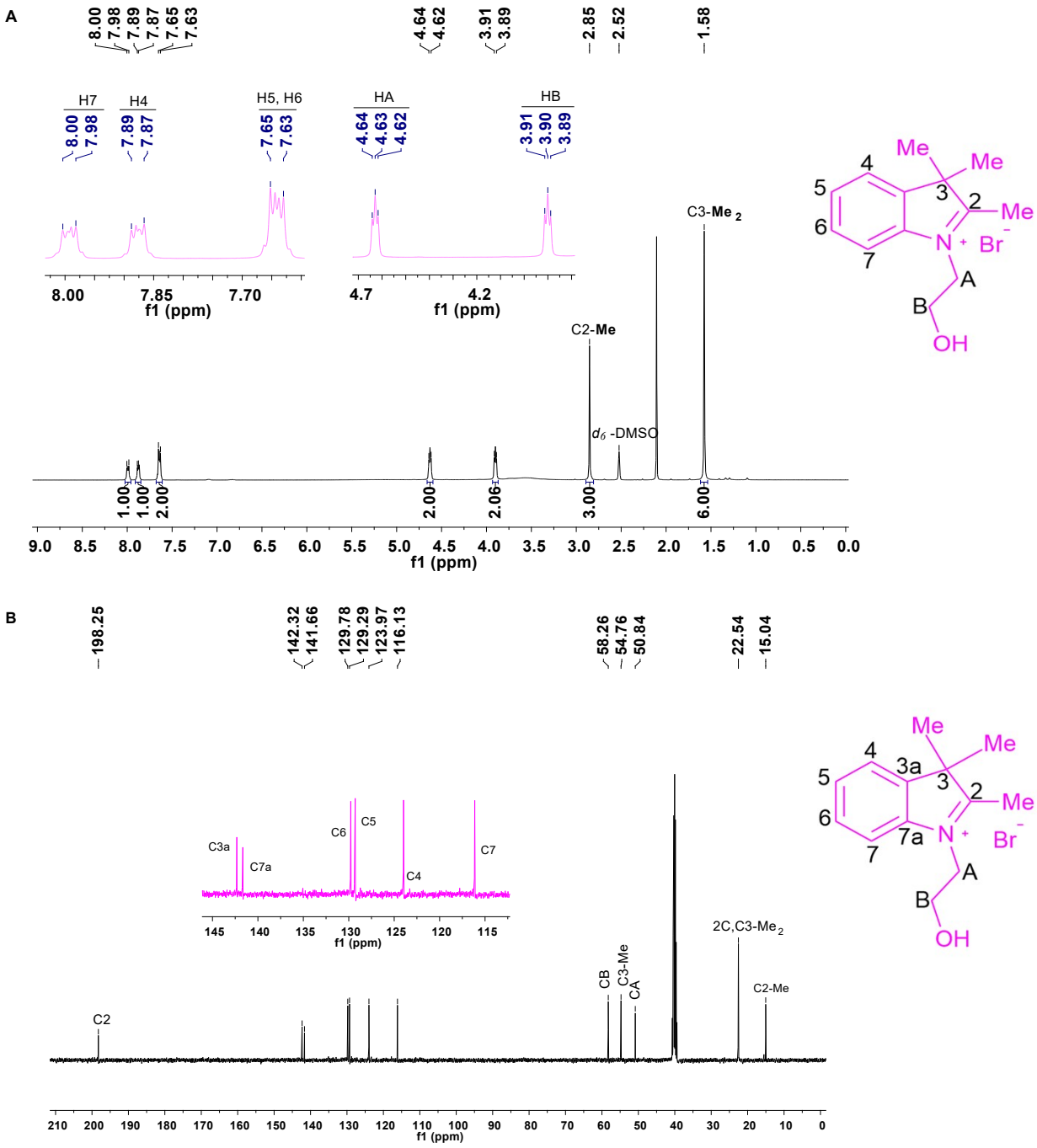

Figure S1. ^{1}H NMR (A) and ^{13}C NMR (B) spectra of Bromide salt in d_6-DMSO.

3.1.2. FT-IR spectrum of Bromide salt

IR (cm^{-1}): 3467 (OH), 3050 ($CH_{2\ (SP^2\ stretch)}$), 2927($CH_{2\ (SP^3 stretch)}$), 1658 (CN^+), 1600 (C=C), 1461 ($CH_{2\ (SP^2\ bend)}$), 1378 ($CH_{2\ (SP^3 bend)}$), 777 ($CH_{\ out\ of\ -plane\ bend}$) (Figure S3).

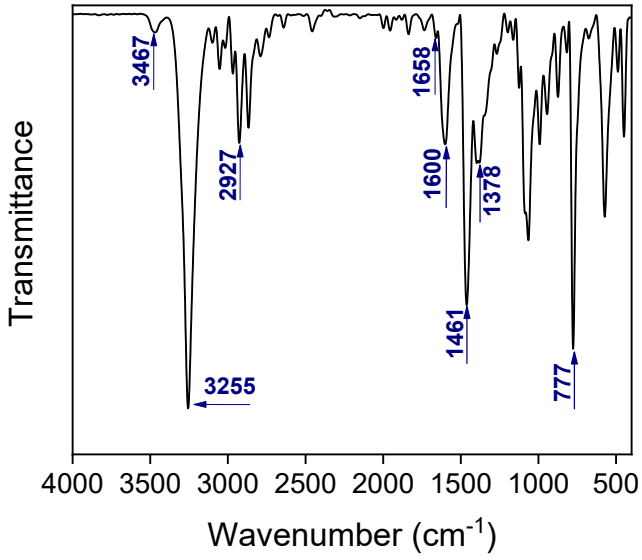

Figure S2. FT-IR spectrum of Bromide salt

3.2. Synthesis of 2-(3',3'-dimethyl-6-nitrospiro[chromene-2,2'-indolin]-1'-yl) ethanol (SP).

Bromide salt (3.8 g, 13.37 mmol) was dissolved in 40 mL of dry ethanol. In one part, piperidine (1.45 mL, 14.67 mmol) and benzaldehyde (3.41 g, 20.4 mmol) were added (Scheme S1). The reaction mixture was refluxed for 6 h. After 6 hours, the purple solution was allowed to reach room temperature and stirred for one additional hour. The product was isolated at 0 ° C, washed with cold ethanol to obtain spiropyran (SP) as violet powder (2.5 g, 84%).
Spiropyran: (352.38 $g.mol^{-1}$, melting point: 168 °C)

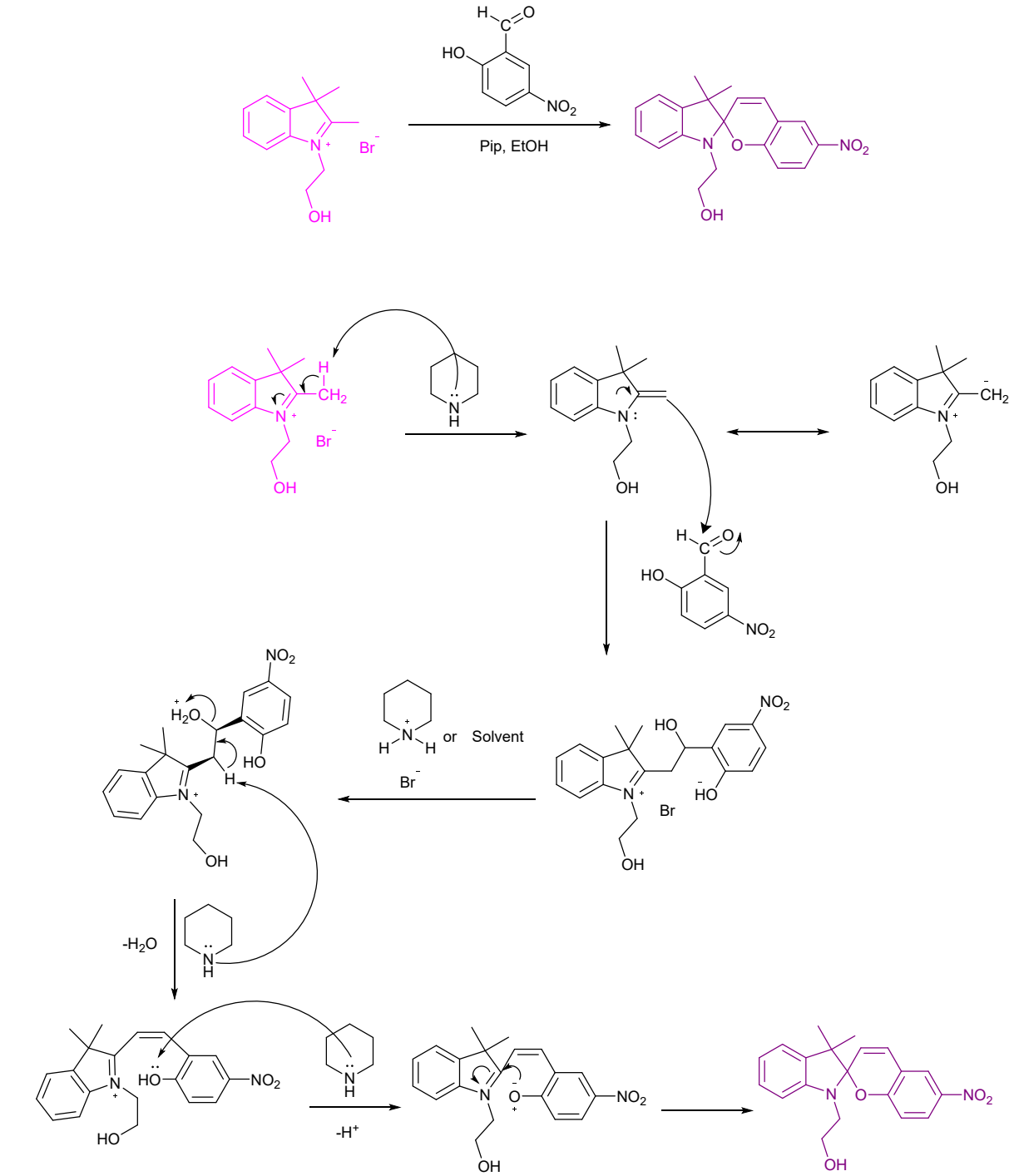

Scheme S3. Synthesis mechanism of 2-(3',3'-dimethyl-6-nitrospiro[chromene-2,2'-indolin]-1'-yl) ethanol (SP)

3.2.1. ^{1}H NMR and ^{13}C NMR of SP

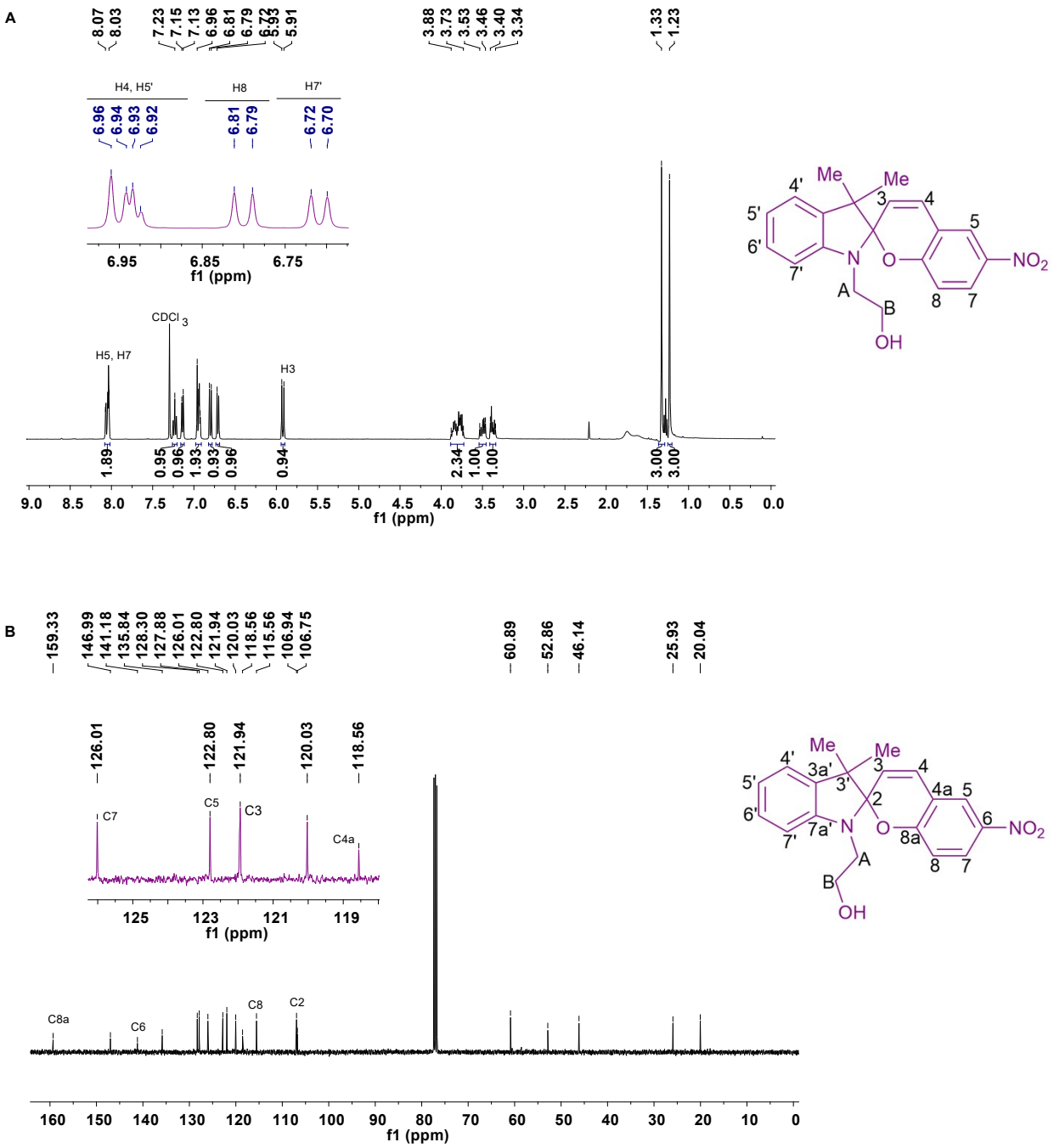

Figure S3. ^{1}H NMR (A) and ^{13}C NMR (B) spectra of SP in $CDCl_3$

3.2.2. FT-IR spectrum of SP

IR (cm^{-1}): 3380 (OH), 3066 ($CH_{2\ (SP^2\ stretch)}$), 2962($CH_{2\ (SP^3 stretch)}$), 1606 and 1479 (C=C), 1509 and 1334 (NO_2), 1087 (C-O), 950 ($CH_{out\ of\text{-}plane\ bend}$) (Figure S4).

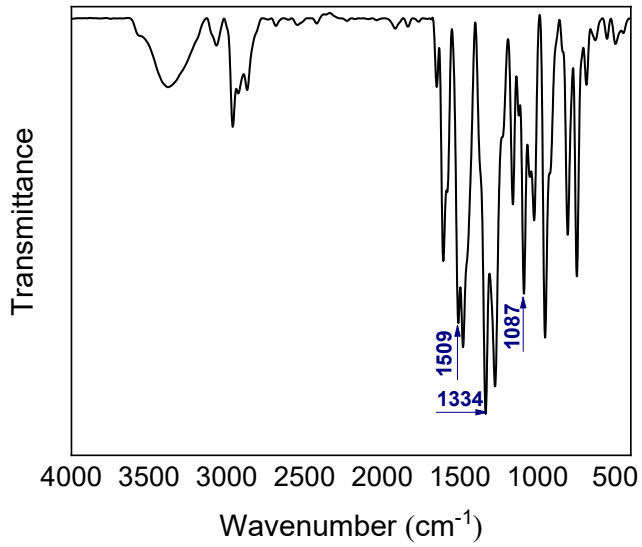

Figure S4. FT-IR spectrum of SP

3.2.3. UV-Vis spectrum of SP

Spiropyran solution with concentration of 2.83×10^{-5} M was prepared in THF, acetonitrile, and ethanol solvents to study the photochromic characteristics of the synthesized compound, and UV-Vis spectra were recorded under irradiation of ultraviolet and visible irradiations. Two planar rings are joined by a common sp^3 hybridized carbon atom in spiropyran type molecules, preventing significant delocalization. As a result, the lowest electronic transition in spiro isomer typically occurs in the near-ultraviolet region.[5] Under UV (λ=365nm) irradiation, the ring opening reaction happens with the cleavage of the C-O spiro bond during the first-order kinetic process, and the two rings combine to create a planar π-conjugation system. As a result, a single delocalized transition has been moved to the visible region. The MC→SP reverse isomerization generally happens according to first-order kinetics, and can be accelerated by visible light. The optical spectra of the spiropyran closed-ring isomer shows two transitions: The π–π* electronic transition in the indoline portion of the molecule is ascribed to the ~ 272–296 nm band, whereas the chromene moiety is attributed to the ~ 323–351 nm band.[6] Solvatochromism is the term used to describe the reversible changes in a chemical compound's UV-Vis absorption spectra (position, intensity, and shape) caused by solute–solvent interactions, especially the polarity of solvents. Environment factors such as hydrogen bonding and polarity of the environment can affect the stability of the merocyanine (MC) isomer. The protic solvent stables the merocyanine isomer, which is due to the strong hydrogen bonding and polarity (Figure S5). In aprotic solvents, there are no suitable interactions between the solvent and MC for hydrogen bonding, and polarity is the controlling factor for solvatochromic behavior of the spiropyran. [7] The MC form is color dependent because to the polarity difference between the photo exited MC and the zwitterionic ground state. For the excited state of the MC form is less polar than the zwitterionic ground state. The ground state of the MC form is stabilized relative to the excited state of the MC form in polar solvents, and leads to more energy gaps than non-polar states. The energy gap between the ground and excited states of MC is reduced by non-polar media that preferentially stabilize the quinoidal form, resulting in a bathochromic shift of the MC band (Figure S6).[6] According to the UV-Vis spectra of Spiropyran after irradiation with UV at 365 nm, in ethanol as protic solvent at 538 nm, in acetonitrile as aprotic polar solvent at 563 nm, and in tetrahydrofuran as semi-polar solvent at 578 nm absorbance of MC has appeared.

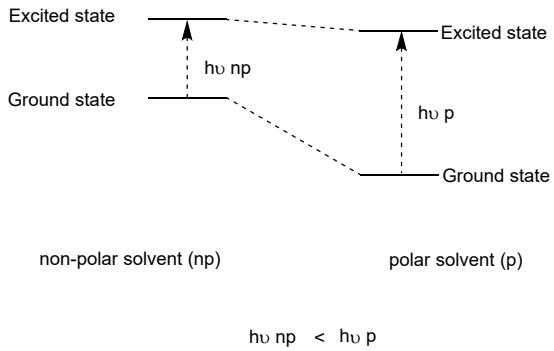

Figure S5. Illustration of the solvatochromic shift of the SP before and after UV irradiation.

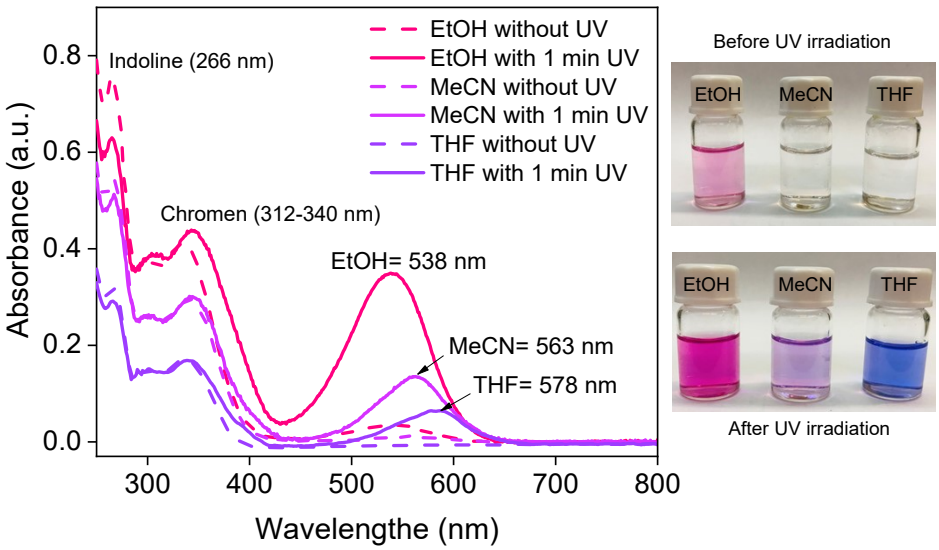

Figure S6. UV-Vis spectra of SP in ethanol, acetonitrile, and THF before and after UV irradiation with 2.83×10^{-5} M concentration.

3.3. Synthesis of 2-(3',3'-dimethyl-6-nitrospiro[chromene-2,2'-indolin]-1'-yl) ethyl acrylate (SPEA).

Spiropyran (2.5 g, 7.09 mmol) was dissolved in dry dichloromethane (23 mL) and the round-bottom flask was isolated with aluminum foil. Then the reaction mixture was cooled to 0 °C and triethylamine (1.25 mL, 10.71 mmol) was added to the solution (Scheme S1). After mixing, acryloyl chloride (0.71 mL, 8.78 mmol) was added dropwise and stirred for one hour at 0 °C. The reaction mixture was stirred at room temperature for 12 hours without stirring. The final product was dissolved in dichloromethane and washed with 0.1 M HCl solution, saturated $NaHCO_3$ solution, and brine. Spiropyran ethylacrylate (SPEA) was isolated as a red sticky substance (0.9 g, 34%).
SPEA: (406.44 g.mol^{-1}, melting point: 98°C)

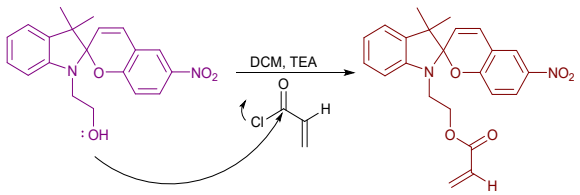

Scheme S4. Synthesis mechanism of 2-(3',3'-dimethyl-6-nitrospiro[chromene-2,2'-indolin]-1'-yl) ethyl acrylate (SPEA).

3.3.1. ^{1}H NMR and ^{13}C NMR of SPEA

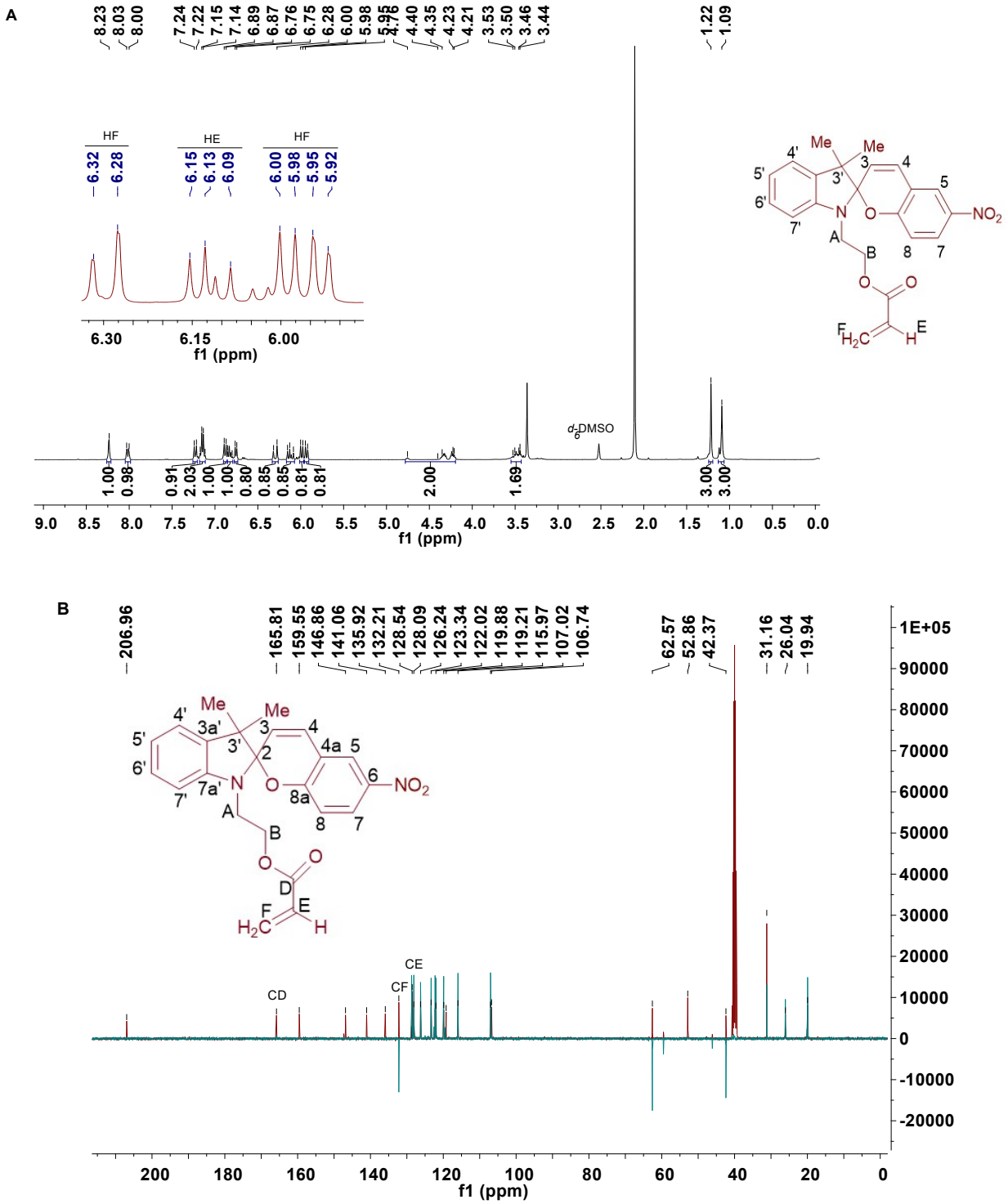

Figure S7. ^{1}H NMR (A) and ^{13}C NMR and DEPT 135 (B) spectra of SPEA in d_6-DMSO.

3.3.2. FT-IR spectrum of SPEA

Evidence of monomer synthesis is the removal of the hydroxyl group adsorption band at 3382 cm^{-1}, and the appearance of a new absorption band at 1725 cm^{-1} corresponding to the ester group (Figure S8).

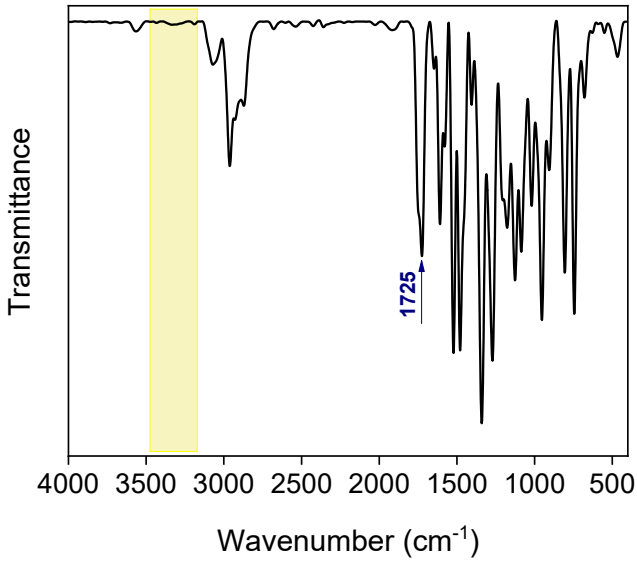

Figure S8. FT-IR spectrum of SPEA

3.3.3. UV-Vis spectra of SPEA

The hydroxyl group of SP compound, which has a lot of polarity, can create hydrogen bonding and induce negative photochromism and solvatochromism. In SPEA, the non-polar acrylate group instead of the hydroxyl group, resulting in decreased in hydrogen bonding formation by the spiropyrane molecule and solvent, lowering negative solvatochromism (Figure S9).

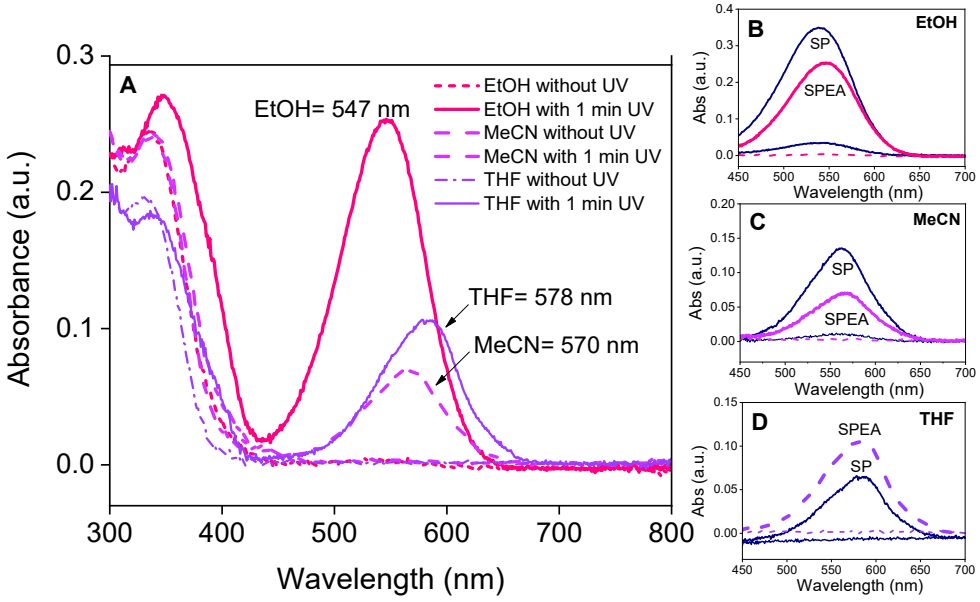

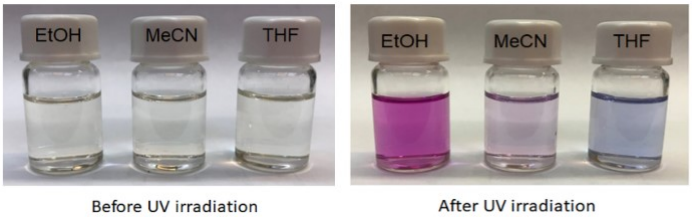

Figure S9. UV-Vis spectra of SPEA in ethanol, acetonitrile and THF before and after UV irradiation with 2.46×10^{-5} M concentration.

4. Surface modification of TiO_2

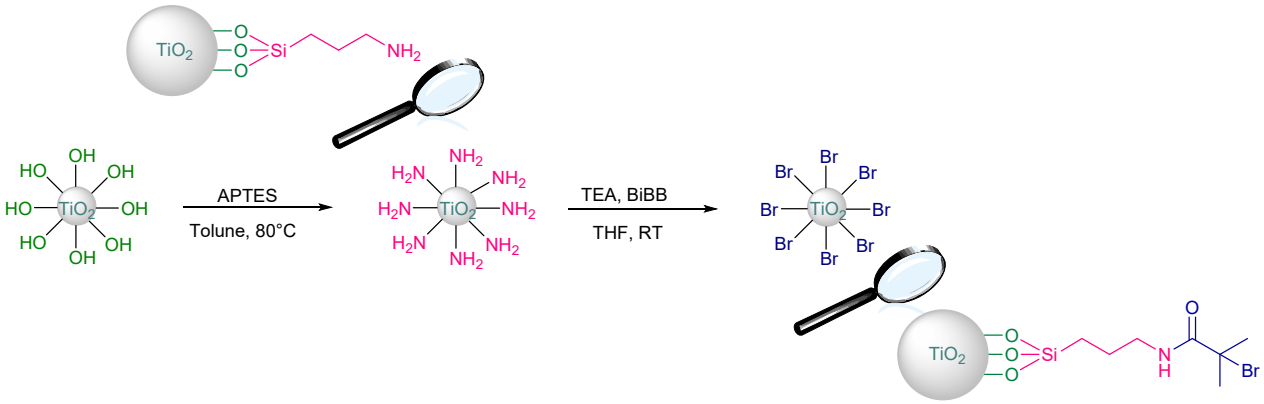

Scheme S5. Surface modification of TiO_2 with APTES and BiBB

4.1. ATRP initiator immobilization on titania surface

Titania nanoparticles (2 g) was refluxed with APTES (6.25 mL, 26.7 mmol) in dry toluene (35 mL) for 24 h and after completion of the reaction, the product was washed with distilled toluene.[8] Under argon atmosphere, THF (19 mL) was added to the modified substrate and homogenized using sonicate bath. The mixture was placed in an ice bath and TEA (1.57 mL, 11.32 mmol) was added and stirred under argon atmosphere for 30 min. BiBB (1.42 mL, 11.49 mmol) was added dropwise to the cold mixture for 30 min, then the reaction was stirred overnight. The resulting precipitate was washed several times with THF and absolute ethanol.[9] (Scheme S5)

4.1.1. FT-IR of TiO_2 P25 nanoparticle

Adsorbed water (intermolecular interactions of water hydroxyl groups with TiO_2 surface) and bending vibrations of hydroxyl groups are related to the wide absorption bands at 3426 and 1629 cm^{-1}, respectively. Ti-O-Ti and Ti-O stretching vibrations are the main absorption bands at 400-700 cm^{-1} (Figure S10).[10, 11]

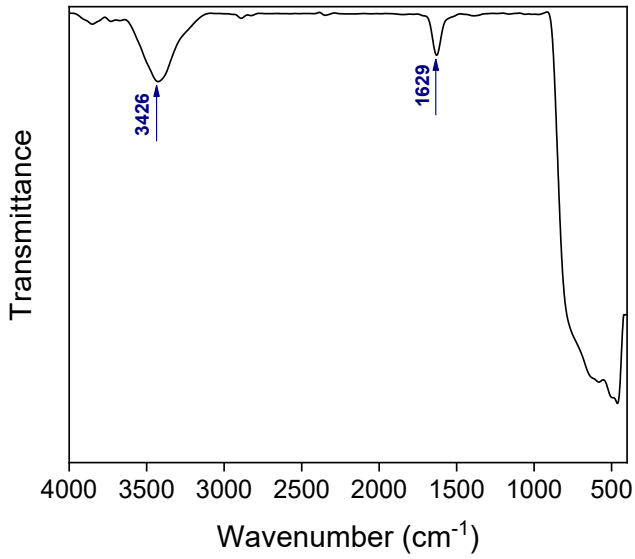

Figure S10. FT-IR spectrum of TiO_2 P25 nanoparticle

4.1.2. TGA and DTG analysis of TiO_2 P25

Weight loss before 120 °C is related to the removal of the adsorbed water. Subsequent weight loss between 120-250 °C is related to the dehydroxylation of adsorbed waters and TiO_2 hydroxyl groups (Figure S11).[11]

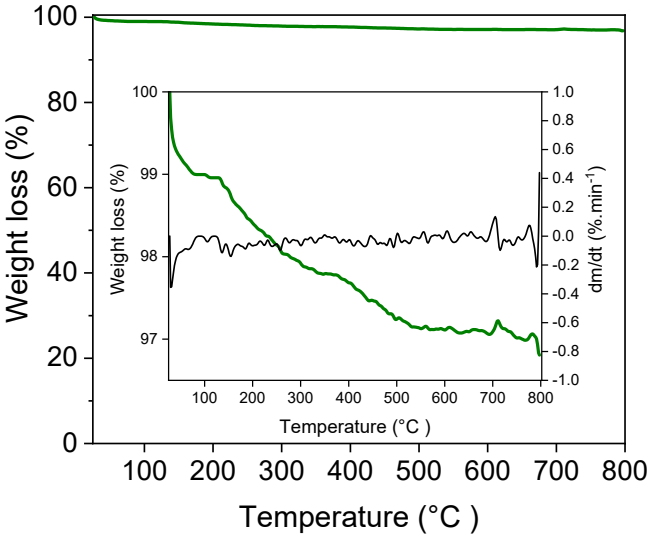

Figure S11. TGA and DTG analysis of TiO_2 P25 in N_2 atmosphere with a heating rate of 10°C/min.

4.1.3. BET of TiO_2 P25 nanoparticle

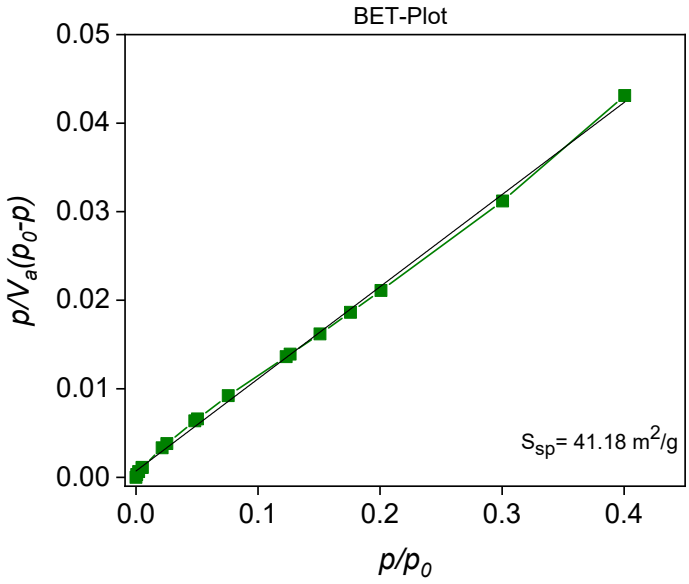

Figure S12. N_2 adsorption-desorption analysis of TiO_2 P25 nanoparticles.

4.1.4. AFM image of TiO_2 P25 nanoparticle

To examine the morphology of the TiO_2 P25 surface, atomic force microscopy (AFM) analysis images were employed. As shown in Figure S13, a considerable aggregation of nanoparticles can be seen.

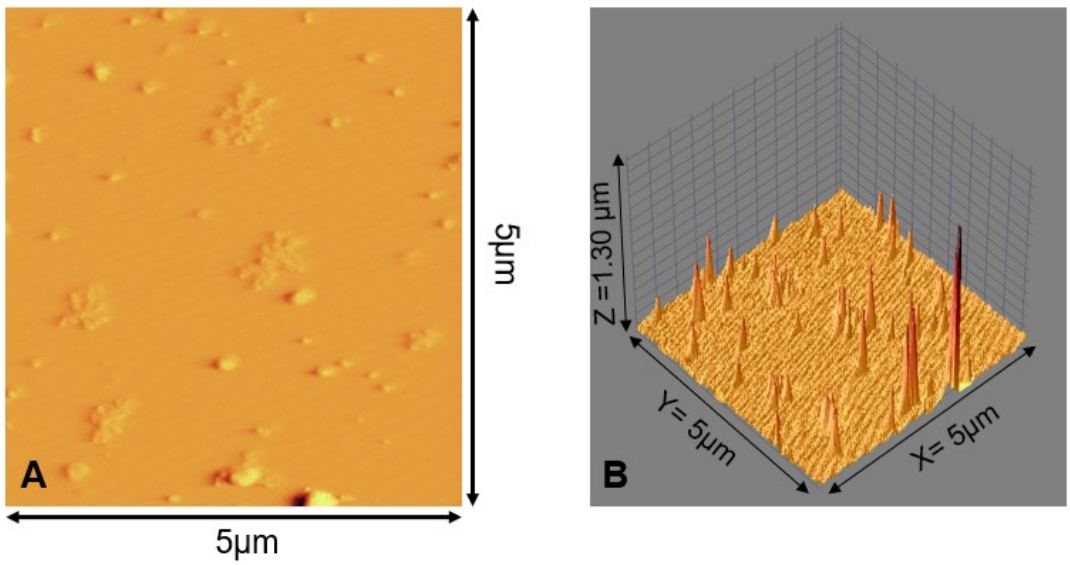

Figure S13. Atomic force microscopy images of TiO_2 P25 (A) two-dimensional (B) three-dimensional.

4.1.5. FT-IR spectrum of TiO_2-NH_2

IR (cm^{-1}): 3423 (O-H, N-H $_{stretch}$), 2913 ([-$(CH_2)_n$-] $_{APTES}$), 1627 ($NH_{2\ bending}$), 1457 (C-H $_{bending}$), 1128 (C-N), 1035 (Si-O-Si) (Figure S14).[12, 13]

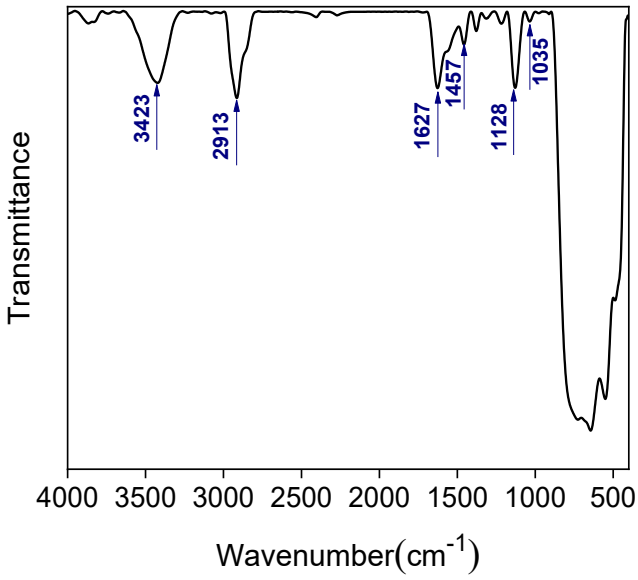

Figure S14. FT-IR spectrum of TiO_2-NH_2

4.1.6. TGA and DTG analysis of TiO_2-NH_2

The first weight loss (2.11%) in the temperature range of 25-250 °C is corresponds to the release of water and other solvents (Figure S15). The second weight loss (1.52%) in the temperature range of 250-450 °C is attributed to the degradation of the organic component, namely aminopropyl and alkyl chains. The final weight loss (3.34%) in the range of 450-800 °C is related to the hydroxylation of the Ti-OH groups remaining on the surface, which leads to the formation of Ti-O-Ti groups. The residual mass (93.02%) is related to the inorganic part of the structure. Due to the second weight loss, the amine content of the titanium dioxide substrate is 0.155 mmol/g.[14]

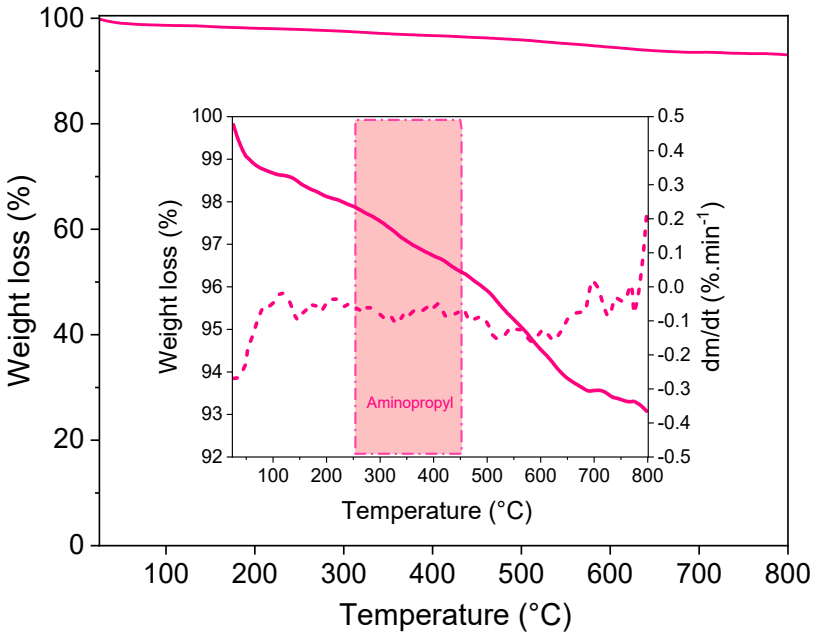

Figure S15. TGA and DTG analysis of TiO_2-NH_2 in N_2 atmosphere with heating rate 10°C/min.

4.1.7. FT-IR spectrum of TiO_2-Br

The new absorption band at 1631 cm^{-1} is related to the stretch vibrations of the C=O group of amides, which is formed by the interactions of the amines on the surface with the α-bromoisobutyral bromide (Figure S16).[15]

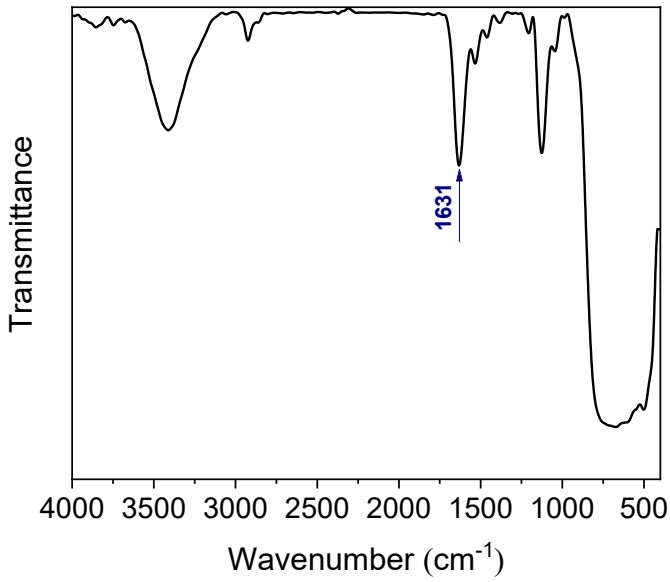

Figure S16. FT-IR spectrum of TiO_2-Br

4.1.8. TGA and DTG analysis of TiO_2-Br

The first and second weight loss (1.44%) in the temperature range of 25-170 °C is related to the release water molecules in the sample. The third weight loss (1.85%) in the temperature range of 170-265 °C was attributed to the degradation of the organic part (initiator). According to the weight loss in the temperature range of 265-450 °C, the amount of Br in the titanium dioxide substrate is 0.222 mmol/g (Figure S17).[16]

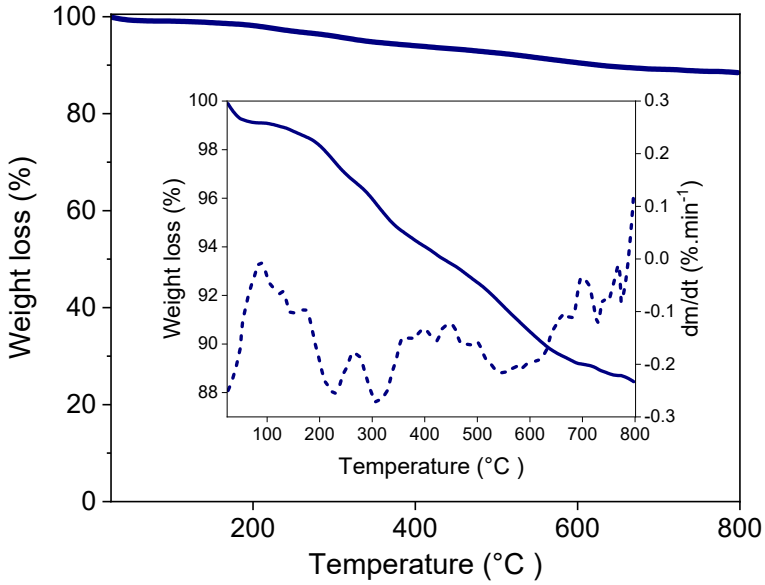

Figure S17. TGA and DTG analysis of TiO_2-Br in N_2 atmosphere with a heating rate of 10°C/min.

4.1.9. BET of TiO_2-Br

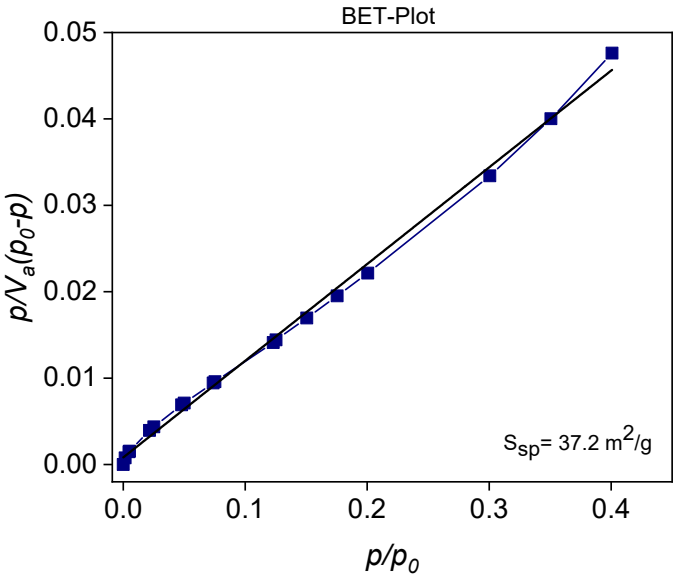

Figure S18. N_2 adsorption-desorption analysis of TiO_2-Br.

Calculations of BET theory showed that the surface area of TiO_2-Br was 37.2 m^2/g (Fig. S19). The decrease in the surface area of TiO_2-Br compared to TiO_2 indicates that the substrate surface has been modified. Based on the results of TGA and BET analysis, the value of 4.74 molecules.nm^{-2} initiator is grafted onto the TiO_2 surface, which is calculated according to the following equation:

$$G_I = \frac{\frac{W\%_{Initiator+TiO2}}{100 - W\%_{Initiator+TiO2}} - \frac{W\%_{TiO2}}{100 - W\%_{TiO2}}}{M_{Initiator} \times S_{sp}} \times N_A \qquad Equation\ 1$$

G_I: initiator grafted density (molecules.nm^{-2})
W%: Weight loss of various nanoparticles from TGA analysis.
N_A: Avogadro's number (6.022×10^{23})
$M_{Initiator}$: Grafted initiator molar mass (149.996 g.mol^{-1})
S_{sp}: Specific surface area. According the BET result, we can know S_{sp} = 37.2×10^{18} $nm^2.g^{-1}$

4.1.10. AFM image of TiO_2-Br

The surface morphology of TiO_2 nanoparticles changed after anchoring the initiator on the surface, and the aggregation of nanoparticles was decreased due to the presence of APTES and BIBB on the surface, according to atomic force microscopy images (Figure S19).

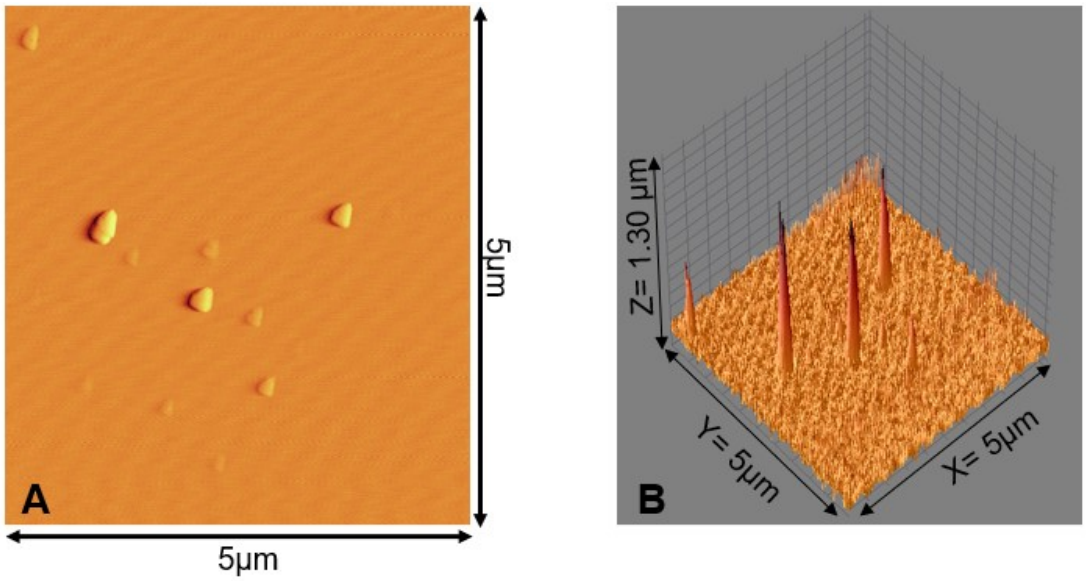

Figure S19. Atomic force microscopy images of TiO_2-Br (A) two-dimensional and (B) three-dimensional.

---

5. Polymer analysis

5.1 Mechanism of polymer grafting via SI-ATRP method

The mechanism for grafting of GMA and SPEA monomers on the surface of the modified TiO_2 nanoparticles is based on ATRP and is shown in the Scheme S6.

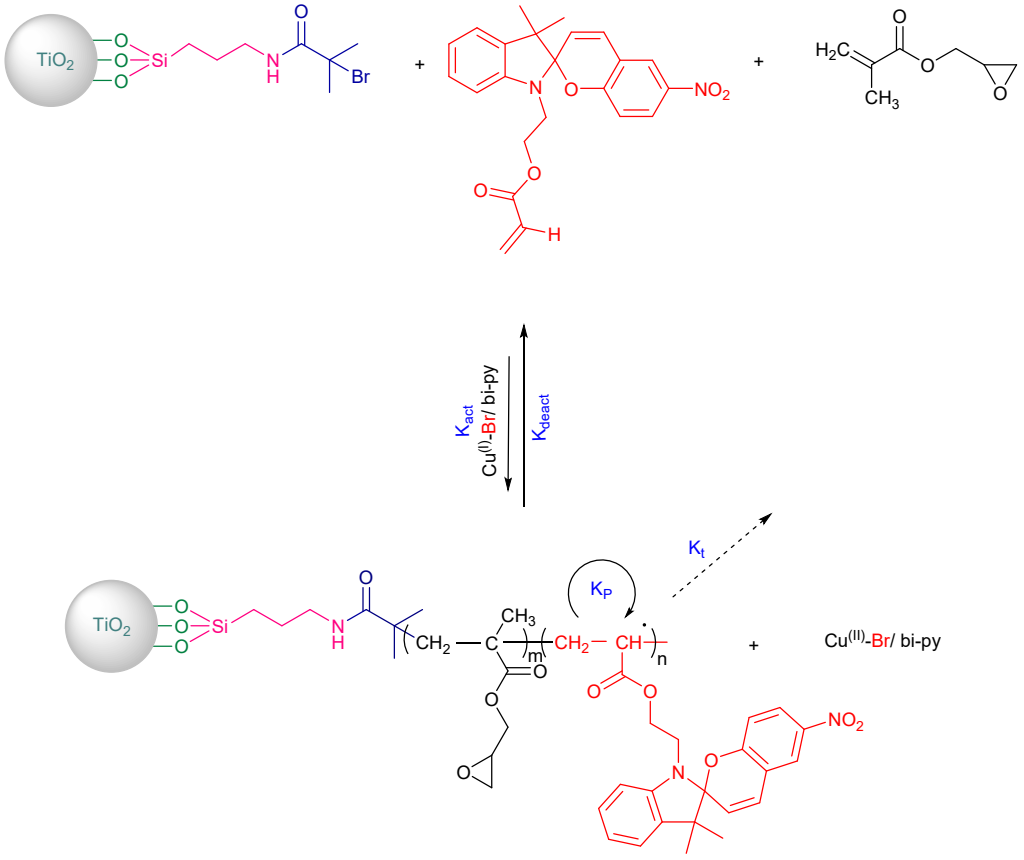

Scheme S6. The mechanism for grafting of GMA and SPEA monomers on the surafec of the modified TiO_2 nanoparticles.

5.2. EDS analysis of TiO_2-*g*-(PSPEA-*co*-GMA)

According to EDS analysis (Figs. S20 A and B), the C, N, and Br content significantly increased after modification of the TiO_2 surface with polymer shows that the surface was successfully modified with photochromic polymer.

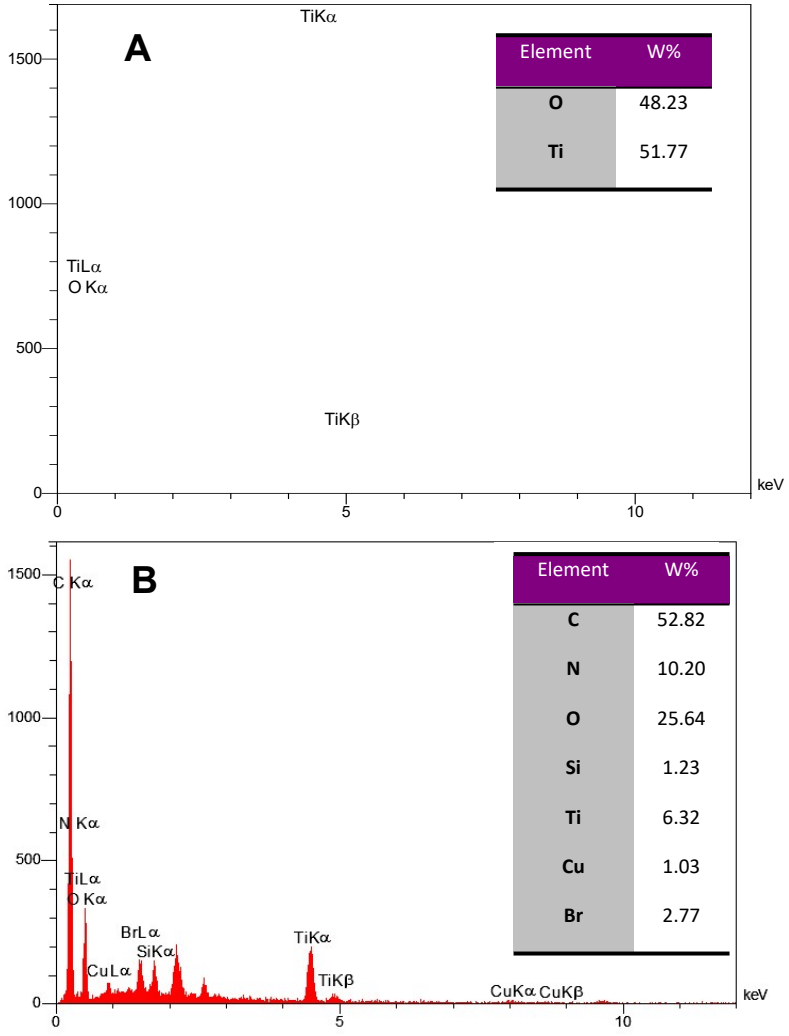

Figure S20. EDS analysis of pure TiO_2 nanoparticles (A) and TiO_2-*g*-P(SPEA-*co*-GMA) (B).

5.3. BET of TiO_2-g-(PSPEA-*co*-GMA)

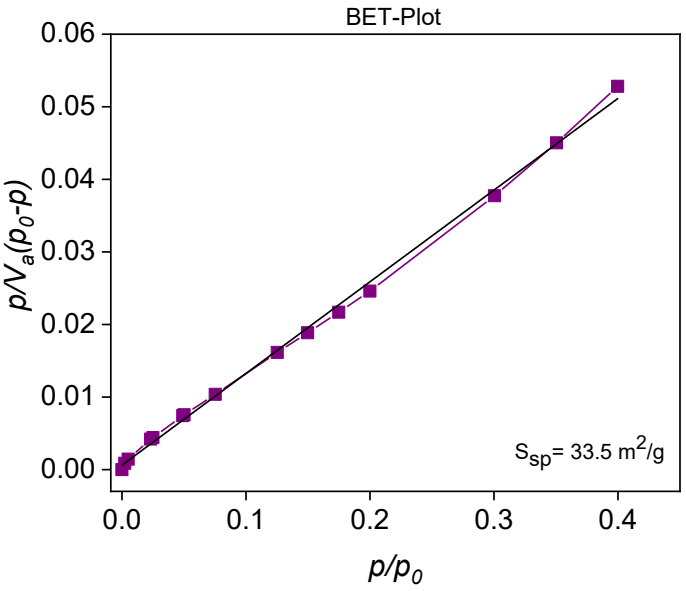

Figure S21. N_2 adsorption-desorption analysis of TiO_2-g-P(SPEA-*co*-GMA).

5.4. UV-Vis spectra of P(SPEA-*co*-GMA) free copolymer

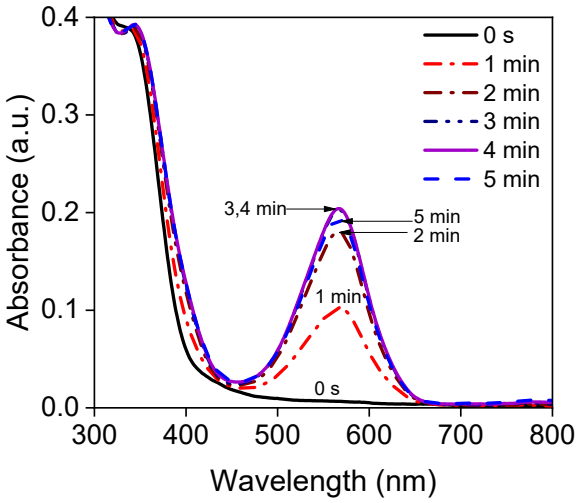

Figure S22. UV-Vis spectra of P(SPEA-*co*-GMA) in acetonitrile at different time intervals.

References

1 W. Armari, *Journal*, 1988.
2 H. C. McCaig, E. Myers, N. S. Lewis and M. L. Roukes, *Nano Lett.*, 2014, **14**, 3728-3732.
3 J. A. Opsteen, R. P. Brinkhuis, R. L. Teeuwen, D. W. Löwik and J. C. van Hest, *Chemical communications*, 2007, 3136-3138.
4 L. Baumann, K. Schöller, D. de Courten, D. Marti, M. Frenz, M. Wolf, R. M. Rossi and L. J. Scherer, *RSC Adv.*, 2013, **3**, 23317-23326.
5 N. A. Murugan, S. Chakrabarti and H. Ågren, *The Journal of Physical Chemistry B*, 2011, **115**, 4025-4032.
6 R. Klajn, *Chem. Soc. Rev.*, 2014, **43**, 148-184.
7 A. Abdollahi, Z. Alinejad and A. R. Mahdavian, *Journal of Materials Chemistry C*, 2017, **5**, 6588-6600.

8 G. Raghuraman, J. Rühe and R. Dhamodharan, *J. Nanopart. Res.*, 2008, **10**, 415-427.
9 L. Xing, N. Guo, Y. Zhang, H. Zhang and J. Liu, *Sep. Purif. Technol.*, 2015, **146**, 50-59.
10 G. Wang, L. Xu, J. Zhang, T. Yin and D. Han, *J. Phot Article ID*, 2012, **265760**.
11 N. C. Martins, J. Ângelo, A. V. Girão, T. Trindade, L. Andrade and A. Mendes, Appl. Catal., B 2016, **193**, 67-74.
12 F. Cheng, S. M. Sajedin, S. M. Kelly, A. F. Lee and A. Kornherr, *Carbohydr. Polym.*, 2014, **114**, 246-252.
13 D. L. Pavia, G. M. Lampman, G. S. Kriz and J. A. Vyvyan, *Introduction to spectroscopy*, Cengage Learning, 2008.
14 M. Sándor, C. L. Nistor, G. Szalontai, R. Stoica, C. A. Nicolae, E. Alexandrescu, J. Fazakas, F. Oancea and D. Donescu, *Materials*, 2016, **9**, 34.
15 L. Liu, H. Chen and F. Yang, *Sep. Purif. Technol.*, 2014, **133**, 22-31.
16 H. Liu, J. Hu, X. Yang, S. Chen and H. Cui, *Des. Monomers Polym.*, 2016, **19**, 193-204.